

RESEARCH ARTICLES

Open Access



Neurovirulent cytokines increase neuronal excitability in a model of coronavirus-induced neuroinflammation

Salil R. Rajayer^{1,2} and Stephen M. Smith^{1,2*}

Abstract

Background Neurological manifestations of severe coronavirus infections, including SARS-CoV-2, are wide-ranging and may persist following virus clearance. Detailed understanding of the underlying changes in brain function may facilitate the identification of therapeutic targets. We directly tested how neocortical function is impacted by the specific panel of cytokines that occur in coronavirus brain infection. Using the whole-cell patch-clamp technique, we determined how the five cytokines (TNF α , IL-1 β , IL-6, IL-12p40 and IL-15 for 22–28-h) at concentrations matched to those elicited by MHV-A59 coronavirus brain infection, affected neuronal function in cultured primary mouse neocortical neurons.

Results We evaluated how acute cytokine exposure affected neuronal excitability (propensity to fire action potentials), membrane properties, and action potential characteristics, as well as sensitivity to changes in extracellular calcium and magnesium (divalent) concentration. Neurovirulent cytokines increased spontaneous excitability and response to low divalent concentration by depolarizing the resting membrane potential and hyperpolarizing the action potential threshold. Evoked excitability was also enhanced by neurovirulent cytokines at physiological divalent concentrations. At low divalent concentrations, the change in evoked excitability was attenuated. One hour after cytokine removal, spontaneous excitability and hyperpolarization of the action potential threshold normalized but membrane depolarization and attenuated divalent-dependent excitability persisted.

Conclusions Coronavirus-associated cytokine exposure increases spontaneous excitability in neocortical neurons, and some of the changes persist after cytokine removal.

Keywords SARS-CoV-2, COVID-19, Neuronal excitability, Neuroinflammation, Delirium, Encephalopathy

Background

Serious neuropsychiatric manifestations of SARS-CoV-2 infection include impaired cognition, altered attentiveness, reduced consciousness, seizures, and abnormal movements [1–4]. The persistence of some neuropsychiatric features beyond clearance of the infection underlines the need for new treatments [4, 5]. The coronavirus-mediated modifications of neuronal activity and connectivity that underlie these acute and chronic clinical changes are unknown. Changes at the single neuron level will alter interneuronal communication and thereby modify the computational properties of circuits and higher level function [6]. Consequently, therapeutic

*Correspondence:
Stephen M. Smith
smisteph@ohsu.edu

¹ Section of Pulmonary, Critical Care, Allergy, and Sleep Medicine, VA Portland Health Care System, 3710 SW U.S. Veterans Hospital Road, R&D 24, Portland, OR 97239, USA

² Department of Medicine, Division of Pulmonary, Allergy and Critical Care Medicine, Oregon Health and Science University, Portland, OR 97239, USA

target identification requires a more detailed understanding of the underlying pathogenesis [7]. Emerging data indicate that neuronal injury in COVID-19 could arise from either sterile inflammation or direct viral infection of the brain [8–12]. The mouse coronavirus, MHV-A59, was utilized as part of an animal model to safely study the actions of the virulent coronaviruses SARS-CoV-1 and MERS-CoV [13]. MHV-A59 is also similar to SARS-CoV-2, as both viruses possess a spike glycoprotein, concentrate in the olfactory mucosa, cause respiratory diseases including ARDS, and lead to acute encephalitis and neuroinflammation [8, 9, 13, 14].

Neuroinflammation, identified by elevated levels of brain cytokines, occurs in COVID-19 and is associated with acute neurological disturbances, persistent structural changes, and severe disease [15–17]. Moreover, markers of neuronal injury such as neuron-specific enolase and S100B correlate with virulence in COVID-19 [18, 19]. MHV-A59 brain infection elevates five proinflammatory cytokines: TNF α , IL-1 β , IL-6, IL-12p40, and IL-15. The cytokine signature differs when coronavirus infects the brain compared to when the virus stays outside the central nervous system [20]. We hypothesized that the specific neurovirulent cytokines (NVC), at concentrations matched to those elicited by MHV-A59 coronavirus infection, would change neuronal function. Our rationale was that determining how neuronal function was altered by NVCs would provide a foundation to later identify druggable targets that may reduce or reverse the neuronal and neurological dysfunction associated with viral neuroinflammation [21]. Neocortical neurons were studied because of the global cortical distribution of inflammation in COVID-19 patients with impaired neurological function [3, 22]. We directly assessed neuronal excitability by studying the frequency of action potentials (APs), the fundamental electrical signal in neurons [23, 24]. A priori it was unclear how NVCs would affect neuronal function overall so we used a range of stimuli to more broadly explore the parameter space of excitability. We examined if NVCs affected the response to a range of current injections as well as reduced extracellular divalent concentration (calcium and magnesium). Decreased extracellular calcium concentration ($[Ca^{2+}]_o$) increases the propensity of neurons to fire APs while reducing the probability of synaptic transmission [29]. Substantial decreases in extracellular calcium occur in association with physiological stimuli and acute neurological insults [25–28]. While viral encephalitis reduces serum calcium and increases extracellular brain levels of calcium-binding proteins [30, 31], it is unclear if brain $[Ca^{2+}]_o$ is significantly reduced by coronavirus infection. We report that NVCs depolarized neurons and increased baseline excitability while simultaneously changing neuronal sensitivity to the microenvironment. Cytokine clearance promptly

normalized baseline excitability without reversing membrane potential depolarization, but the changes in sensitivity to the microenvironment were more complex. The loss of sensitivity to divalents persisted for evoked activity, while spontaneous response to decreased divalents was substantially attenuated following cytokine clearance. These data indicate that at least two mechanisms underlie the changes in neuronal function following exposure to coronavirus-associated cytokines.

Methods

Primary neocortical cultures

All animal procedures were approved by VA Portland Health Care System Institutional Animal Care and Use Committee in accordance with the U.S. Public Health Service Policy on Humane Care and Use of Laboratory Animals and the National Institutes of Health Guide for the Care and Use of Laboratory Animals (IRBNetID: 1,659,311, Protocol 4359-20). Neocortical neurons were isolated from 1- to 2-day-old mice of both sexes from a stable breeding colony of wild-type C57BL/6JX129X1 mice as described previously [32]. Briefly, animals were decapitated following anesthesia with isoflurane and cerebral cortices were removed. Cortices were incubated in trypsin and DNase (5 mg/mL and 0.1 mg/mL for 5 min at 34° C) and dissociated with heat polished pipettes. Dissociated cells were maintained in Minimum Essential Medium with Earle's balanced salt solution (MEM/EBSS, HyClone Labs, South Logan, UT) plus 5% fetal bovine serum (FBS) on glass coverslips in an incubator (humidified air and 5% CO₂) at 37° C. Cytosine arabinoside (4 μ M) was added 48–72 h after plating to limit glial division. Cells were used after 10–30 days in culture.

Preparation of neurovirulent cytokines

NVC cytokines were applied at final concentrations described in Table 1 below. These levels were selected to match average values measured in astrocytes infected with MHV-A59 for TNF α , IL-6 and IL-12p40 [20]. The concentrations of IL-1 β and IL-15 were estimated by multiplying basal values by the expression level ratios for control and infected cells. NVC stock solution was prepared immediately prior to application and contained all cytokines at 100 or 1000-times the final concentrations listed in Table 1 below combined in water. The individual stock solutions used to prepare the NVC solution were made by dissolving lyophilized cytokines (Peprotech, NJ) in MEM plus 5%

Table 1 Neurovirulent cytokine concentrations (pg/ml) used

Cytokine	TNF- α	IL-1 β	IL-6	IL-12 p40	IL-15
Conc. (pg/ml)	185	400	380	690	1

FBS or water plus 0.1% BSA at 0.1–0.5 µg/µL and stored at –80 °C in individual aliquots. In control experiments, equivalent solutions minus the cytokines were used to treat the cultures.

Electrophysiological recordings

Adjacent coverslips on the same culture plate were treated with NVC solution (1% or 0.1% v/v) or vehicle control (0.0002% BSA) for 22–28 h after which the coverslips were transferred to a recording chamber and continuously perfused with extracellular Tyrode solution ($\text{Ca}_{1.1}$) containing (in mM): 150 NaCl, 4 KCl, 10 HEPES, 10 glucose, 1.1 MgCl_2 , 1.1 CaCl_2 , pH corrected to 7.35 with NaOH. Solutions were applied by gravity from a glass capillary (1.2 mm outer diameter) placed 1–2 mm from the neuron under study. Recordings were made using an amplifier (Heka EPC10, Lambrecht, Pfalz, Germany) and 5–10 MΩ resistance electrodes. Recordings were filtered at 2.9 kHz and acquired by digitizing at 20 kHz. Approximately 5 min after establishing whole-cell configuration and balancing the amplifier circuits, neurons were subjected to current injection protocols as described in individual experiments. Recordings were made in $\text{Ca}_{1.1}$ prior to switching over to a similar solution with reduced divalents ($\text{Ca}_{0.2}$, 0.2 mM CaCl_2 and MgCl_2). The patch electrode contained the following (in mM): 135 K-gluconate, 10 HEPES, 4 MgCl_2 , 0.3 NaGTP, 4 NaATP, 10 phosphocreatine disodium, pH corrected to 7.20 with KOH. All reagents were supplied by Sigma-Aldrich (St. Louis, MO). Voltages were corrected for liquid junction potentials. Experiments were performed at 21–23° C.

Statistical analysis

Analysis was performed using Igor Pro (Wavemetrics, OR). APs were identified as brief deflections from the resting membrane potential (RMP) that peaked at or above –20 mV. AP threshold was measured as the point at which dV/dt reached 40 mV/ms (see Supplemental Figure s3A). AP amplitude was defined as the voltage difference between membrane potential and peak. AP half-width was defined as the time between rising and falling phases of the AP, measured at the midpoint between the peak and membrane potential. To standardize the approach and minimize variation, measurements were restricted to the first AP elicited by a 40 pA injection. Only neurons that fired APs in both $\text{Ca}_{1.1}$ and $\text{Ca}_{0.2}$ were subject to analysis of AP characteristics in order to enable paired analysis. All data values were reported as mean ($\pm \text{SE}$). Statistical tests were performed using IBM SPSS v28 or GraphPad Prism 9. Data from control and NVC-treated neurons at $\text{Ca}_{1.1}$ and $\text{Ca}_{0.2}$ were analyzed using two-way repeat measures ANOVA. For groups exhibiting a significant interaction between divalent change and

NVC treatment ($P < 0.05$), we performed simple main effects analysis. If there was no interaction, we analyzed the individual group differences (NVC or divalents) independently. Post hoc tests were performed when appropriate by Sidak's multiple comparison tests. For analyzing contingencies, such as comparing the likelihood of neurons staying electrically silent, we used the Fisher exact test. For comparing two individual groups, we used the Student's *t*-test.

Microarray analysis of gene expression in neocortical cultures

Data from microarray analysis used to characterize RNA expression levels of receptors for cytokines in these cultures are available at NCBI GEO (GSE218028) [33] and shown in Additional file 1: Table S1.

Results

NVC increases spontaneous excitability

Action potentials are transient membrane depolarizations that propagate along neuronal processes and may evoke synaptic transmission, a major form of interneuronal communication. The propensity of neurons to generate APs (excitability) can be evaluated by measuring AP frequency [23, 24]. APs occur when changes in membrane conductance, usually due to presynaptic release of neurotransmitter, depolarize the membrane potential to threshold. Initially, we tested if NVC incubation changed the propensity to fire spontaneous APs under resting conditions. In neurons at resting membrane potential, activity was low and 13/42 neurons (31%) fired APs spontaneously over a 100-s period. NVC-treated neurons were more excitable, and 18/24 (75%) fired APs over the same time ($P = 0.0008$, Fisher's exact test).

We next tested how reduced extracellular divalent concentration affected neuronal excitability, because decreases in external calcium change brain activity in physiological and pathophysiological conditions [25–28]. We counted the spontaneously occurring APs acquired over 100 s in physiological solution ($\text{Ca}_{1.1}$), and after reducing extracellular divalent concentrations ($\text{Ca}_{0.2}$, Fig. 1A). NVC treatment ($P = 0.017$) and reduced divalent concentration ($P < 0.0001$) both substantially increased AP firing with no interaction (Fig. 1B). Our finding that NVC treatment increases the likelihood of AP generation, indicates neuroinflammatory cytokines change the functional properties of neocortical neurons.

Usually, lowered extracellular divalent concentration increases neuronal excitability, in part, by facilitating activation of voltage-gated sodium channels (VGSCs) and depolarizing the membrane potential [32]. NVC treatment substantially depolarized RMP in $\text{Ca}_{1.1}$ (Fig. 1C, $P = 0.025$) and $\text{Ca}_{0.2}$ ($P < 0.0001$). The independent variables

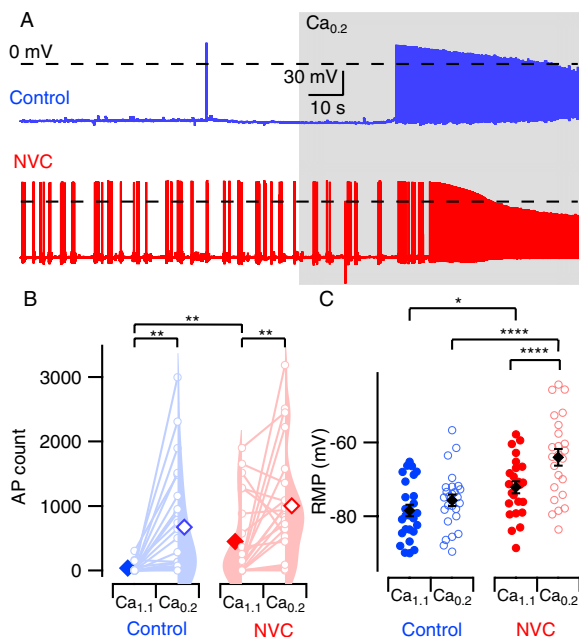


Fig. 1 NVC increases spontaneous excitability. **A** Representative voltage tracers of spontaneous APs. Blue represents control and red, NVC. Shaded area indicates Ca_{0,2}. Each trace represents 160 s of continuous acquisition. **B** Violin density plots (shaded) showing total AP count at 100 s in Ca_{1,1} and Ca_{0,2}. Paired values represented by connected open circles showing change in AP count following divalent switch from Ca_{1,1} to Ca_{0,2}. Diamonds indicate mean values, solid Ca_{1,1} and open Ca_{0,2}. Mean AP counts in control were 35 ± 15 in Ca_{1,1}, increasing to 670 ± 170 in Ca_{0,2}. NVC exposure increased AP counts in Ca_{1,1} to 448 ± 131 and 1002 ± 182 in Ca_{0,2}. Two-way repeated measures (RM) ANOVA suggested no interaction between divalent reduction and NVC ($F(1,45) = 0.099$, $P = 0.753$). However, both divalents ($P < 0.0001$) and NVC ($P = 0.017$) independently increased AP counts. Post hoc testing with Sidak multiple comparisons reveals divalent change increased firing in both control ($P = 0.001$) and NVC ($P = 0.004$). NVC increased AP firing at Ca_{1,1} ($P = 0.002$) but not Ca_{0,2} ($P = 0.190$), $N = 24$ (control) and 23 (NVC), respectively. **C** Plot with individual values of RMP. RMP in control was -78.4 ± 1.5 mV in Ca_{1,1} and -75.7 ± 1.5 mV in Ca_{0,2}. NVC treatment depolarized neurons to -72.1 ± 1.6 mV in Ca_{1,1} and -64.0 ± 2.3 mV in Ca_{0,2}. Solid circles represent Ca_{1,1} and open circles, Ca_{0,2}. Two-way RM ANOVA indicates that divalent reduction and NVC treatment interact to depolarize RMP ($F(1,48) = 6.281$, $P = 0.016$). Post hoc testing with Sidak multiple comparisons reveals that NVC depolarizes RMP at both Ca_{1,1} ($P = 0.025$) and Ca_{0,2} ($P < 0.0001$). $N = 26$ (control) and 24 (NVC). Solid diamonds with error bars represent mean \pm SEM. Control indicated by blue and NVC, red. Statistically significant P-values in this figure and all others denoted by schema * < 0.05 , ** < 0.01 , *** < 0.001 and **** < 0.0001

interacted such that NVC increased the divalent-dependent depolarization ($P = 0.016$). The enhanced sensitivity to divalents was also illustrated by comparing RMP depolarization upon switching to Ca_{0,2} (2.7 ± 1.1 mV and 8.1 ± 1.9 mV for control and NVC-treated neurons, respectively, $P = 0.019$, Additional file 1: Fig. S1A). NVC

and Ca_{0,2} depolarized the membrane potential towards the AP threshold, presumably contributing to the observed increase in excitability. This may arise due to shifts in VGSC gating or activation of other membrane conductances [32, 34–36].

NVC clearance rapidly restores baseline spontaneous activity

We evaluated if NVC-mediated changes in neuronal function were affected by the removal of cytokines. The fraction of neurons in which spontaneous APs were recorded ~1 h after clearance of NVC (NVC_c), was similar to control ($P > 0.99$, 5/15 (33%) of NVC_c and 13/42 (31%) of control neurons). Similarly, NVC_c reduced the total number of APs generated in Ca_{1,1} in contrast to sustained NVC treatment (Fig. 2B). However, NVC_c-treated neurons were surprisingly different to both control and NVC-treated neurons in terms of their sensitivity to external divalent concentration. In NVC_c-treated neurons, application of Ca_{0,2} did not change AP count (Fig. 2B; $P = 0.99$), which contrasted with control and NVC-treated neurons (Figs. 1B, 2B). In NVC_c-treated neurons, cytokines and reduced divalents both independently depolarized the RMP (Fig. 2C, $P < 0.0001$, $P = 0.0004$) as observed with NVC treatment (Fig. 1C). However, the lack of an interaction between cytokines and reduced divalents represented another difference between NVC- and NVC_c-treated neurons (Supplemental Figure s1). The loss of exaggerated depolarization with the switch to low divalent levels in the NVC_c-treated neurons, is likely to contribute to the coincident change in divalent-dependent excitability. Overall, while NVC_c-treated neurons exhibited reduced $[Ca^{2+}]_o$ -dependent excitability, the NVC-mediated changes in RMP persisted.

NVC attenuates divalent-dependent increase in evoked APs

In addition to counting spontaneous APs, neuronal excitability can be evaluated by eliciting APs with depolarizing currents [37]. This approach may enhance our ability to detect decreases in excitability by increasing the basal activity. We injected depolarizing currents from RMP and the number of APs increased with current amplitude and Ca_{0,2} as expected for control neurons (Fig. 3A, B, [32]). NVC treatment did not affect neuronal excitability when assessed by the number of APs elicited by current injections (Fig. 3C, $P = 0.91$), in contrast to its action on spontaneous activity (Fig. 1B). Overall, lowering the external divalent concentration increased the AP count ($P = 0.0008$) but this was confined to control neurons (Fig. 3C, $P = 0.0005$). This attenuation of evoked divalent-dependent excitability in NVC-treated neurons

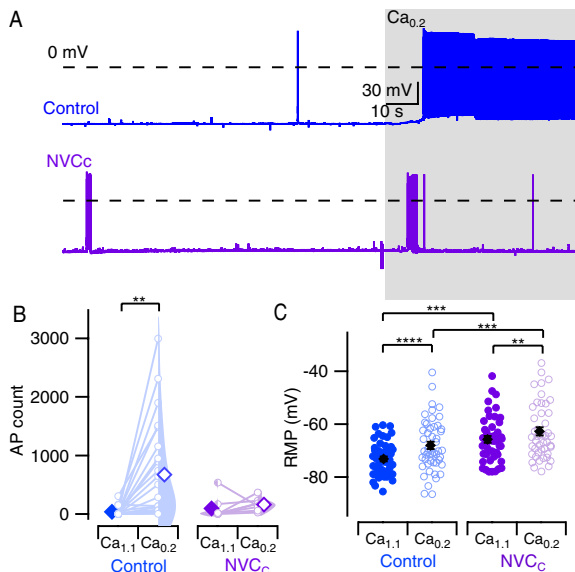


Fig. 2 NVC clearance rapidly restores baseline spontaneous activity. **A** Representative voltage tracers for recordings of spontaneous action potentials. Blue tracers represent control and purple NVC clearance (NVC_c). Shaded area represents application of Ca_{0,2}. **B** Violin plots showing distribution of total AP count at 100 s in Ca_{1,1} and Ca_{0,2} in control and NVC_c, schema similar to Fig. 1B. Mean AP counts in control were 35 ± 15 in Ca_{1,1}, increasing to 670 ± 170 in Ca_{0,2}. AP counts following NVC_c in Ca_{1,1} and 92.4 ± 66 and 159.1 ± 37.7 in Ca_{0,2}. Two-way RM ANOVA did not indicate an interaction between divalent change and NVC_c ($P=0.063$) although decreasing divalents had an overall effect ($P=0.024$). While change in divalents increased spontaneous AP firing in control ($P=0.0013$), there was no similar increase noted following NVC_c ($P=0.99$, $N=24$ and 8, for control and NVC_c, respectively). **C** Plots with individual values and mean of RMP. Blue denotes control and purple, NVC_c. Individual values represented by solid circles (Ca_{1,1}) and open circles (Ca_{0,2}). Solid diamonds represent mean values. Mean ± SE for RMP in control; Ca_{1,1} = -73.1 ± 0.9 mV and Ca_{0,2} = -68.0 ± 1.4 mV, in NVC_c; Ca_{1,1} = -65.7 ± 1.3 mV and Ca_{0,2} = -62.8 ± 1.5 mV. Two-way RM ANOVA indicates that divalent levels and NVC_c had no interaction ($F(1,93)=2.578$, $P=0.112$), but both NVC_c ($P=0.0004$) and divalent reduction ($P<0.0001$) had independent effects. Post hoc testing with Sidak multiple comparisons reveals that RMP was depolarized by NVC_c at both Ca_{1,1} ($P=0.0002$) and Ca_{0,2} ($P=0.009$). $N=49$ and 46 for control and NVC_c, respectively.

contrasted with our observations on spontaneous activity (Fig. 1 and Additional file 1: S1). The membrane potential deflection appeared reduced following current injection in the NVC-treated neurons consistent with a reduced input resistance. However, measurement of the voltage deflection elicited by -20 pA injections revealed the trend towards a lower input resistance was non-significant ($P=0.269$, Additional file 1: Fig. S2A).

We next examined if cytokine removal affected evoked excitability. NVCc-treated cells were insensitive to the switch from Ca_{1,1} to Ca_{0,2} when assessed by current

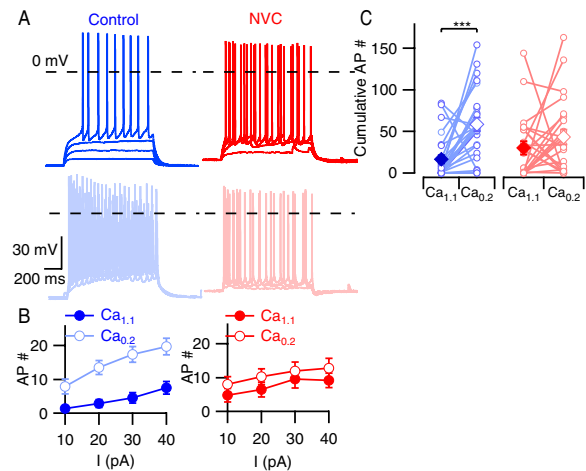


Fig. 3 NVC attenuates divalent-dependent increase in evoked APs. **A** Exemplar traces showing AP firing following incremental 1 s current injections of 10–40 pA from RMP. Blue represents control and red NVC. Dark tracers represent Ca_{1,1} and light Ca_{0,2}. **B** Graphs showing average AP count in control (blue) and NVC (red), measurements in Ca_{1,1} (solid, filled circles) and Ca_{0,2} (faint, open circles) represented by separate lines. Error bars represent standard error. Mean AP counts in control Ca_{1,1} = 7.5 ± 1.8 and increase to 19.7 ± 2.4 in control Ca_{0,2} at 40 pA, whereas NVC AP counts at the same current injections ranged from 9.2 ± 2.1 at NVC Ca_{1,1} to 12.8 ± 2.9 at NVC Ca_{0,2}. **C** Plot showing average cumulative elicited AP count in control (blue) and NVC (red) for each recording. Mean values for Ca_{1,1} represented by solid diamonds and Ca_{0,2} by open diamonds. Mean values for control Ca_{1,1} and Ca_{0,2} were 16.5 ± 5.1 and 58.6 ± 8.0, whereas NVC Ca_{1,1} and Ca_{0,2} were 30.2 ± 7.6 and 43.1 ± 9.0, respectively. Individual values represented by open circles connected by a line showing change in cumulative AP count following switch from Ca_{1,1} to Ca_{0,2}. Error bars represent standard error. Comparison by two-way RM ANOVA shows no interaction between divalent concentration and NVC treatment ($F(1,48)=3.616$, $P=0.06$) or independent effect of NVC ($P=0.91$) but decreasing divalents had an effect ($P=0.0008$). Post hoc analysis with Sidak multiple comparisons shows different effects in control and NVC, with increase in average cumulative AP count in control ($P=0.0005$) but no effect of NVC ($P=0.436$). $N=26$ and 24 for control and NVC groups

injection (Fig. 4A–C) similar to NVC-treated neurons (Fig. 3). In addition, both NVC- and NVCc-treated neurons showed trends towards increased basal activity in Ca_{1,1}. Taken together, these data indicate that the impact of NVC on excitability depends on the approach used to measure excitability.

NVC transiently modifies AP threshold

There are many mechanisms by which changes in AP shape elicit short- and long-term alterations in neuronal excitability [23, 24, 38]. We tested how AP characteristics were affected by NVC treatment. The effects of NVC treatment and external divalent concentration on AP threshold interacted (Fig. 5A) [32]. As expected, AP

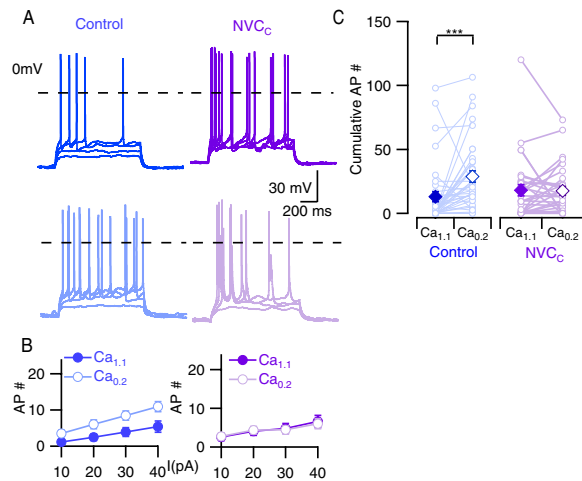


Fig. 4 Evoked divalent-dependent excitability remains attenuated after NVC clearance. **A** Exemplar traces showing AP firing following incremental 1-s current injections of 10–40 pA from RMP. Blue represents control and purple NVC clearance (NVC_c). Dark tracers represent Ca_{1,1} and light Ca_{0,2}. **B** Graphs showing average AP count in control (blue) and NVC_c (purple), measurements in Ca_{1,1} (solid, filled circles) and Ca_{0,2} (faint, open circles) represented by separate lines. Error bars represent standard error. 40 pA current injections in control elicited 5.4 ± 1.5 APs in Ca_{1,1} and 10.9 ± 1.3 APs in Ca_{0,2} whereas NVC_c elicited 6.6 ± 1.5 APs in Ca_{1,1} and 6.0 ± 1.3 APs in Ca_{0,2}. **C** Plot showing average cumulative AP count for each recording. Schema similar to Fig. 3C. Control Ca_{1,1} and Ca_{0,2} = 12.9 ± 4.0 and 28.9 ± 4.4 , whereas NVC_c Ca_{1,1} and Ca_{0,2} = 18.1 ± 4.4 and 17.61 ± 3.4 , respectively. Two-way RM ANOVA showing an interaction between divalent concentration and NVC_c ($F(1,66) = 7.820, P = 0.006$). Simple main effects analysis showed there was no independent effect of NVC_c ($P = 0.544$) but divalent concentration had an independent effect ($P = 0.010$). Post hoc analysis by Sidak multiple comparisons confirmed divalent-dependent increase in excitability was present in control ($P = 0.003$) but not in NVC_c ($P = 0.99$). $N = 37$ and 31 for control and NVC_c groups

threshold was hyperpolarized by Ca_{0,2} in control neurons [32]. In NVC-treated neurons, the AP threshold was relatively hyperpolarized in Ca_{1,1} and unaffected by the switch to Ca_{0,2} (Fig. 5A). Shifts in RMP and threshold will both impact excitability because spike generation is more likely when the gap between RMP and AP threshold decreases which may account for the divalent-dependent evoked excitability in controls (Fig. 3A). However, in NVC-treated neurons there was no significant change in the number of APs following the switch from Ca_{1,1} to Ca_{0,2} (Fig. 3C) despite the relatively hyperpolarized AP threshold and depolarized RMP.

Cytokine-mediated changes to AP threshold were quickly reversed following NVC clearance. AP thresholds (Fig. 5B) were indistinguishable in control and NVC_c groups and were similarly hyperpolarized by lowering divalent levels ($P = 0.004$ and 0.041 for control and NVC_c, respectively). In NVC_c-treated neurons, the absence of

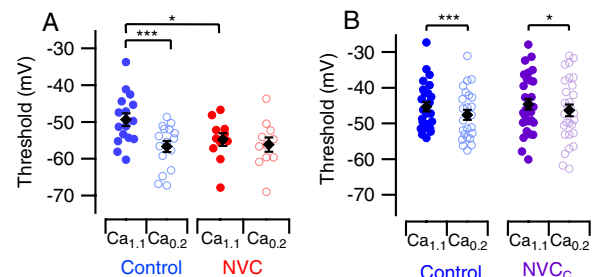


Fig. 5 NVC transiently modifies AP threshold. **A** Plot of AP threshold, color schema similar to Fig. 1C. Mean \pm SE values for control Ca_{1,1} vs. Ca_{0,2} = -49.3 ± 1.7 mV vs. -56.6 ± 1.5 mV and NVC Ca_{1,1} vs. Ca_{0,2} = -54.8 ± 1.7 mV vs. -56.1 ± 1.9 mV. Two-way RM ANOVA indicates that both divalent levels and NVC interact to hyperpolarize the AP threshold ($F(1,25) = 5.99, P = 0.022$). Post hoc testing with Sidak multiple comparisons shows hyperpolarization of AP threshold at Ca_{1,1} between control and NVC ($P = 0.042$), but this effect is absent at Ca_{0,2} ($P = 0.835$). In addition, divalent change hyperpolarized AP threshold in control ($P < 0.001$) but not NVC cells ($P = 0.481$). **B** Plot of AP threshold, color schema similar to Fig. 2C. Mean \pm SE values for control Ca_{1,1} vs. Ca_{0,2} = -45.3 ± 1.3 mV vs. -47.6 ± 1.3 mV and NVC_c Ca_{1,1} vs. Ca_{0,2} = -44.6 ± 1.5 mV vs. -46.3 ± 1.6 mV. Two-way RM ANOVA indicates that divalent levels and NVC_c do not interact to change AP threshold ($F(1,52) = 0.667, P = 0.418$), but divalent change had an independent effect ($P < 0.001$). Post hoc testing with Sidak multiple comparisons shows divalent change hyperpolarized AP threshold in both control ($P = 0.004$) and NVC_c cells ($P = 0.041$)

divalent-dependent excitability (Fig. 4) despite the divalent sensitivity of AP threshold (Fig. 5B) indicates that AP threshold changes do not explain the cytokine-generated alterations in excitability. NVC did not independently affect AP amplitude ($P = 0.281$) and AP half-maximal width ($P = 0.796$, Additional file 1: Fig. S3) and NVC_c had no independent effect on AP amplitude ($P = 0.082$) and AP half-maximal width ($P = 0.473$, Additional file 1: Fig. S4B, C).

Discussion

Using the MHV-A59 model, originally developed to study the SARS and MERS coronaviruses, we investigated the action of a specific panel of NVCs on neocortical neurons. Our major finding was that day-long exposure to the specific panel of NVCs produced an average 12.8-fold increase in the likelihood of spontaneous action potential generation (Fig. 1B). Despite this large increase in excitability, NVC-treated neurons retained their ability to detect and respond to decreases of the divalent ion concentration in the extracellular environment (Fig. 1B). However, divalent-dependent excitability was lost by NVC-treatment when the APs were elicited by current injection (Fig. 3). We also determined that NVCs depolarized the resting membrane potential, increased the sensitivity of the membrane potential to

decreased $[Ca^{2+}]_o$ and hyperpolarized the AP threshold. Only the effects of NVCs on resting membrane potential and evoked divalent-dependent excitability persisted after cytokine removal (Figs. 2C, 4C). Otherwise, NVC_C-treated cells and control neurons were indistinguishable except for the unexpected loss of spontaneous divalent-dependent excitability (Fig. 2).

It is not immediately apparent how NVC application caused these many changes in neuronal function and how the changes interacted. The action of low divalents was studied because $[Ca^{2+}]_o$ decreases by 30–90% during times of high neuronal activity and following acute neurological insult [25–28], and this stimulus modifies neuronal excitability [32, 37, 39]. As mentioned above, we hypothesized that incorporation of $[Ca^{2+}]_o$ as a parameter would expand our study of the effects of NVC, but we were surprised by their different effects on spontaneous and evoked excitability (Figs. 1, 3). Previously, spontaneous and evoked APs were both used as fairly equivalent measures of excitability [32, 40]. In our recordings, the evoked APs occurred as a result of experimental depolarizations (1 s), whereas spontaneous APs were more likely to result from synaptic inputs. Consequently, the enhanced effect of NVC on spontaneously measured excitability may have arisen if NVCs were acting in part, by increasing excitatory synaptic transmission. Another important finding was the rapid reduction in spontaneous excitability to control levels only one hour after NVC removal (Fig. 2B). On its own, this suggested the impact of NVCs on neuronal function was rapidly reversible consistent with a direct pharmacological effect. However, the associated loss of calcium-dependent excitability (Fig. 2B) indicated some additional sustained effects of NVCs. Persistent effects were also apparent in the experiments evaluating evoked excitability after NVC clearance (Fig. 4B) which were indistinguishable from those where NVCs were not removed. Our evaluation of excitability under a range of conditions, point to two or more mechanisms working together, and that one causes effects that persist for at least an hour after NVC clearance.

NVC depolarized the RMP, hyperpolarized the AP threshold, and increased divalent-dependent depolarization (Fig. 1C, 5A). The changes in RMP and AP threshold both reduced the voltage deflection required to trigger an AP following a depolarizing synaptic input. The heightened sensitivity of the RMP to decreased extracellular divalent concentrations also increased neuronal excitability by further depolarizing the neuron towards the AP threshold. The increase in synaptic activity, hypothesized to explain the pronounced effects on spontaneous excitability (Fig. 1) could arise as a result of changes in RMP, AP threshold, calcium-dependent excitability or represent a distinct action of cytokines. The measured increases in

excitability, were all expected to alter the input–output functions of individual neurons, increase the likelihood of AP-evoked synaptic transmission, modify the computational properties of circuits and consequently, behaviors [41–43].

A key finding was the apparent stability of the NVC-induced changes in RMP (Figs. 1C, 2C), contrasting with the reversibility of the changes in AP threshold (Fig. 5), and may point to the mechanisms behind the changes in excitability. Using this approach, the reversal of spontaneous activity in $Ca_{1.1}$ could reflect the change in AP threshold with NVC clearance, whereas the sustained changes in evoked calcium-regulated excitability could depend on the largely intact NVC-mediated changes in RMP. Further complexity is indicated by the complete loss of spontaneous calcium-dependent excitability after NVC clearance which starkly contrasts with the intact calcium-dependent excitability after sustained NVC-treatment. In addition, it may be necessary to invoke downregulation of synaptic activity as a result of cytokine induced homeostatic plasticity [44] to explain the rapid switch from heightened to absent calcium-dependent excitability in the NVC- and NVC_C-treated neurons.

We have not yet experimentally addressed the mechanisms of action of NVC on neuronal function. The transient effects of NVC on RMP depolarization, AP threshold, and excitability could have arisen in a number of ways. The VGSC is an important candidate because a gating shift could increase channel availability, resulting in an increase in persistent VGSC currents, hyperpolarization of the AP threshold, and an increase in the likelihood of AP generation [32]. This would also explain the enhanced depolarization following the switch to $Ca_{0.2}$ as divalent-dependent depolarization is mainly due to increased VGSC current in these neurons [32]. VGSC regulation by GPCRs and intracellular messengers usually increases VGSC inactivation [45, 46] so the observed NVC actions would require reversal of one of these pathways [47] or a counteracting mechanism [48]. Mechanisms that may contribute to the observed transient effects of NVCs, also include functional changes in one or more other ion channels. For instance, reduced potassium channel activity, including the two-pore leak channels, or increased non-selective channel activity, such as hyperpolarization-activated, cyclic nucleotide gated channel (HCN), at baseline, would depolarize the neurons and increase the likelihood of AP generation. The change in AP threshold might also be attributable to potassium channel closure, while increased divalent sensitivity of the RMP could reflect upregulation of a $[Ca^{2+}]_o$ -sensitive non-selective cation channel such as calcium homeostasis modulator (CALHM1) [36] or the sodium leak channel non-selective protein NALCN [35].

In addition to these post-synaptic mechanisms, enhanced excitatory synaptic transmission could also contribute to the transient effects of NVC by increasing the likelihood of AP generation. The persistent effects of NVC treatment observed after NVC clearance may have arisen from changes in expression levels of membrane proteins that impact the RMP. Candidates include many of the channels listed above as well as the sodium–potassium-ATPase pump. Interest in a potential role for some of these targets is heightened by reports linking their regulation by neuroinflammation. Inhibition of HCN channels has known anti-inflammatory effects [49], while CALHM1 and potassium channels are thought to be activated by inflammation [50]. Future experiments will focus on determining the involvement of these candidate mechanisms in the regulation of excitability by NVCs in order to identify therapeutic targets.

Neuropsychiatric illnesses occur during and following infection with coronaviruses and are important contributors to the morbidity of the COVID-19 pandemic. Inflammation of the brain and the associated encephalopathy may occur early in the disease course, especially in the setting of severe illness [1–3], and present as delirium. Using the MHV-A59 model, originally developed to study severe coronavirus infections, we determined that the viral cytokine signature substantially changed neuronal function. If we were to speculate about the clinical implications of this study, then the changes in neuronal function during (NVC) cytokine application could represent the changes underlying acute illnesses such as delirium or encephalopathy. Likewise, the changes observed in the NVC_C-treated neurons might explain post-viral illnesses such as long-COVID. Other viral illnesses have also been associated with neuroinflammation, clinical seizures, and chronic neurodegeneration [51, 52]. While there is some overlap in the types of cytokine that are elevated in the various viral encephalitides, it is clear that a distinct group of cytokines has not been identified as responsible for the neuropsychiatric manifestations of all types of viral illness [52, 53]. Individually cytokines have a multiplicity of actions on neuronal function [54, 55], and it is unclear if the cytokine signatures of other viruses would alter neuronal function in the same ways as the NVCs we utilized here. However, the increased neuronal excitability we observed with sustained cytokine exposure, could feasibly predispose to seizures, a common clinical manifestation of encephalitis.

Intrinsic neuronal function and synaptic transmission in the primary neocortical culture share many properties with those observed in the acute brain slice [24, 56] supporting our use of this preparation here. Moreover, the neocortical culture expresses receptors to the NVC panel (Table 1) and its use facilitated the direct and safe testing

of how neuronal function was affected by prolonged exposure to the cytokine signature of a coronavirus CNS infection [20]. However, an *in vivo* model remains an important next step to directly study the pathogenesis of SARS-CoV-2-associated delirium and encephalopathy as it would facilitate the linking of changes in neuronal function with altered behavior. Such a model would also enable studies to determine if the effects of NVCs changed with neurodevelopment. Addressing these limitations, would better position us to identify and test plausible druggable targets to reduce the dysfunction associated with coronavirus neuroinflammation. Another question raised by the study is whether similar changes in neuronal excitability occur with other types of infection? The answer will help determine if the mechanisms underlying neuropsychiatric manifestations of other infections overlap. Finally, experiments extending the duration of exposure with NVC are required to begin understanding the consequences of prolonged neuroinflammation arising from SARS-CoV-2 infection.

Conclusions

In conclusion, we have described the changes in neuronal function that occur following exposure to the cytokine signature of a serious central coronavirus infection. This dysfunction was partially reversible and included a substantial increase in excitability, altered sensitivity to changes in the extracellular microenvironment, and depolarization of the resting membrane potential.

Supplementary Information

The online version contains supplementary material available at <https://doi.org/10.1186/s40635-023-00557-9>.

Additional file 1: Figure S1. NVC mediated increase in divalent-dependent depolarization is reversible following NVC clearance. **Figure S2.** Input Resistance of neurons is not altered by NVC or NVC clearance. **Figure S3.** AP Amplitude and AP Half-maximal width are sensitive to divalent change but not NVC. **Figure S4.** AP Amplitude and AP Half-maximal width are unchanged following NVC clearance. **Table S1.** Microarray analysis of cell culture characteristics and cytokine receptors.

Acknowledgements

We thank Mr. Luke Steiger, Ms. Maya Feldhouse, Ms. Sophia Klein, Ms. Jamie Lindner and Dr. Timur Tsintsadze for helpful discussions. We thank Dr.s Jeff Gold, Gary Westbrook, and Stefan Hallermann for their comments on earlier drafts of the manuscript.

Author contributions

SRR participated in research design, conducted the experiments, performed data analysis and wrote the first draft of the manuscript. SMS participated in the research design, performed data analysis, edited the first draft and contributed substantially to the writing of the manuscript.

Funding

This work was supported by grants awarded by NIGMS (GM134110) and U.S. Department of Veterans Affairs (BX002547) to SMS and MRF (ECI1021099) and NHLBI (T32HL083808) to SRR. The contents do not represent the views of the

U.S. Department of Veterans Affairs or the United States Government. The authors do not report any additional conflicts of interest.

Availability of data and materials

The datasets used and/or analyzed during the current study are available from the corresponding author on reasonable request.

Declarations

Ethics approval and consent to participate

All animal procedures were approved by Veterans Affairs Portland Health Care System Institutional Animal Care and Use Committee in accordance with the United States Public Health Service Policy on Humane Care and Use of Laboratory Animals and the National Institutes of Health Guide for the Care and Use of Laboratory Animals (IRBNetID: 1659311, Protocols 4359–20).

Consent for publication

Not applicable.

Competing interests

The authors declare that they have no competing interests.

Received: 10 August 2023 Accepted: 4 October 2023

Published online: 14 October 2023

References

- Mao L, Jin H, Wang M, Hu Y, Chen S, He Q, Chang J, Hong C, Zhou Y, Wang D, Miao X, Li Y, Hu B (2020) Neurologic manifestations of hospitalized patients with coronavirus disease 2019 in Wuhan, China. *JAMA Neurol* 77:683–690
- Dias R, Caldas JP, Silva-Pinto A, Costa A, Sarmento A, Santos L (2022) Delirium severity in critical patients with COVID-19 from an infectious disease intensive care unit. *Int J Infect Dis* 118:109–115
- Helms J, Kremer S, Merdji H, Schenck M, Severac F, Clere-Jehl R, Studer A, Radosavljevic M, Kummerlen C, Monnier A, Boulay C, Fafi-Kremer S, Castelain V, Ohana M, Anheim M, Schneider F, Meziani F (2020) Delirium and encephalopathy in severe COVID-19: a cohort analysis of ICU patients. *Crit Care* 24:491
- Xu E, Xie Y, Al-Aly Z (2022) Long-term neurologic outcomes of COVID-19. *Nat Med* 28:2406–2415
- Spudich S, Nath A (2022) Nervous system consequences of COVID-19. *Science* 375:267–269
- Cook ND (2008) The neuron-level phenomena underlying cognition and consciousness: synaptic activity and the action potential. *Neuroscience* 153:556–570
- Mukerji SS, Solomon IH (2021) What can we learn from brain autopsies in COVID-19? *Neurosci Lett* 742:135528
- Song E, Zhang C, Israelow B, Lu-Culligan A, Prado AV, Skriabine S, Lu P, Weizman OE, Liu F, Dai Y, Szegedi-Buck K, Yasumoto Y, Wang G, Castaldi C, Heltke J, Ng E, Wheeler J, Alfajaro MM, Levavasseur E, Fontes B, Ravindra NG, Van Dijk D, Mane S, Gunel M, Ring A, Kazmi SAJ, Zhang K, Wilen CB, Horvath TL, Plu I, Haik S, Thomas JL, Louvi A, Farhadian SF, Huttner A, Seilhean D, Renier N, Bilguvar K, Iwasaki A (2021) Neuroinvasion of SARS-CoV-2 in human and mouse brain. *J Exp Med*. 2021;218(3):e20202135. <https://doi.org/10.1084/jem.20202135>.
- Vidal E, López-Figueroa C, Rodon J, Pérez M, Brustolin M, Cantero G, Gualar V, Izquierdo-Useros N, Carrillo J, Blanco J, Clotet B, Vergara-Alert J, Segalés J (2022) Chronological brain lesions after SARS-CoV-2 infection in hACE2-transgenic mice. *Vet Pathol* 59:613–626
- Seehusen F, Clark JJ, Sharma P, Bentley EG, Kirby A, Subramaniam K, Wunderlin-Giuliani S, Hughes GL, Patterson EL, Michael BD, Owen A, Hiscox JA, Stewart JP, Kipar A (2022) Neuroinvasion and neurotropism by SARS-CoV-2 variants in the K18-hACE2 mouse. *Viruses*. 14(5):1020. <https://doi.org/10.3390/v14051020>
- Crunfli F, Carregari VC, Veras FP, Silva LS, Nogueira MH, Antunes A, Vendramini PH, Valença AGF, Brandão-Teles C, Zucoli GDS, Reis-de-Oliveira G, Silva-Costa LC, Saia-Cereda VM, Smith BJ, Codo AC, de Souza GF, Muraro SP, Parise PL, Toledo-Torres DA, Santos de Castro ÍM, Melo BM, Almeida GM, Firmo EMS, Paiva IM, Silva BMS, Guimarães RM, Mendes ND, Ludwig RL, Ruiz GP, Knittel TL, Davanzo GG, Gerhardt JA, Rodrigues PB, Forato J, Amorim MR, Brunetti NS, Martini MC, Benatti MN, Batah SS, Siyuan L, João RB, Aventurato ÍK, Rabelo de Brito M, Mendes MJ, da Costa BA, Alvim MKM, da Silva Júnior JR, Damiao LL, de Sousa IMP, da Rocha ED, Gonçalves SM, Lopes da Silva LH, Bettini V, Campos BM, Ludwig G, Tavares LA, Pontelli MC, Viana RMM, Martins RB, Vieira AS, Alves-Filho JC, Arruda E, Podolsky-Gondim GG, Santos MV, Neder L, Damasio A, Rehen S, Vinolo MAR, Munhoz CD, Louzada-Junior P, Oliveira RD, Cunha FQ, Nakaya HI, Mauad T, Duarte-Neto AN, Ferraz da Silva LF, Dolnikoff M, Saldiva PHN, Farias AS, Cendes F, Moraes-Vieira PMM, Fabro AT, Sebollela A, Proenca-Modena JL, Yasuda CL, Mori MA, Cunha TM, Martins-de-Souza D (2022) Morphological, cellular, and molecular basis of brain infection in COVID-19 patients. *Proc Natl Acad Sci U S A* 119:e2200960119
- Pattanaik A, Bhandarkar BS, Lohda L, Marate S (2023) SARS-CoV-2 and the nervous system: current perspectives. *Arch Virol* 168:171
- Yang Z, Du J, Chen G, Zhao J, Yang X, Su L, Cheng G, Tang H (2014) Coronavirus MHV-A59 infects the lung and causes severe pneumonia in C57BL/6 mice. *Virol Sin* 29:393–402
- Bender SJ, Weiss SR (2010) Pathogenesis of murine coronavirus in the central nervous system. *J Neuroimmune Pharmacol* 5:336–354
- Wu Y, Xu X, Chen Z, Duan J, Hashimoto K, Yang L, Liu C, Yang C (2020) Nervous system involvement after infection with COVID-19 and other coronaviruses. *Brain Behav Immun* 87:18–22
- McElvaney OJ, McEvoy NL, McElvaney OF, Carroll TP, Murphy MP, Dunleavy DM, Choileán ON, Clarke J, O'Connor E, Hogan G, Ryan D, Sulaiman I, Gunaratnam C, Branagan P, O'Brien ME, Morgan RK, Costello RW, Hurley K, Walsh S, Barra Ed, McNally C, McConkey S, Boland F, Galvin S, Kiernan F, O'Rourke J, Dwyer R, Power M, Geoghegan P, Larkin C, O'Leary RA, Freeman J, Gaffney A, Marsh B, Curley GF, McElvaney NG. Characterization of the inflammatory response to severe COVID-19 illness. *Am J Respir Crit Care Med*. 2020; 202: 812–821.
- Mandel M, Harari G, Gurevich M, Achiron A (2020) Cytokine prediction of mortality in COVID19 patients. *Cytokine* 134:155190
- Aceti A, Margarucci LM, Scaramucci E, Orsini M, Salerno G, Di Sante G, Gianfranceschi G, Di Liddo R, Valeriani F, Ria F, Simmaco M, Parnigotto PP, Vitali M, Romano Spica V, Michetti F (2020) Serum S100B protein as a marker of severity in Covid-19 patients. *Sci Rep* 10:18665
- Silva RC, da Rosa MM, Leão HI, Silva EDL, Ferreira NT, Albuquerque APB, Duarte GS, Siqueira AM, Pereira MC, Rêgo M, Pitta MGR (2023) Brain damage serum biomarkers induced by COVID-19 in patients from northeast Brazil. *J Neurovirol* 29:180–186
- Li Y, Fu L, Gonzales DM, Lavi E (2004) Coronavirus neurovirulence correlates with the ability of the virus to induce proinflammatory cytokine signals from astrocytes and microglia. *J Virol* 78:3398–3406
- Ising C, Heneka MT (2018) Functional and structural damage of neurons by innate immune mechanisms during neurodegeneration. *Cell Death Dis* 9:120
- Lersy F, Bund C, Anheim M, Mondino M, Noblet V, Lazzara S, Phillips C, Collange O, Oulehri W, Mertes PM, Helms J, Merdji H, Schenck M, Schneider F, Pottecher J, Giraudeau C, Chammas A, Ardellier FD, Baloglu S, Ambarki K, Namer IJ, Kremer S (2022) Evolution of neuroimaging findings in severe COVID-19 patients with initial neurological impairment: an observational study. *Viruses*. 14(5):949. <https://doi.org/10.3390/v14050949>
- Bean BP (2007) The action potential in mammalian central neurons. *Nat Rev Neurosci* 8:451–465
- Ritzau-Jost A, Tsintsadze T, Krueger M, Ader J, Bechmann I, Eilers J, Barbour B, Smith SM, Hallermann S (2021) Large, stable spikes exhibit differential broadening in excitatory and inhibitory neocortical boutons. *Cell Rep* 34:108612
- Nicholson C, ten Bruggencate G, Stöckle H, Steinberg R (1978) Calcium and potassium changes in extracellular microenvironment of cat cerebellar cortex. *J Neurophysiol* 41:1026–1039
- Nilsson P, Hillered L, Olsson Y, Sheardown MJ, Hansen AJ (1993) Regional changes in interstitial K⁺ and Ca²⁺ levels following cortical compression contusion trauma in rats. *J Cereb Blood Flow Metab* 13:183–192

27. Puka-Sundvall M, Hagberg H, Andine P (1994) Changes in extracellular calcium concentration in the immature rat cerebral cortex during anoxia are not influenced by MK-801. *Brain Res Dev Brain Res* 77:146–150
28. Zhang ET, Hansen AJ, Wieloch T, Lauritzen M (1990) Influence of MK-801 on brain extracellular calcium and potassium activities in severe hypoglycemia. *J Cereb Blood Flow Metab* 10:136–139
29. Jones BL, Smith SM (2016) Calcium-sensing receptor: a key target for extracellular calcium signaling in neurons. *Front Physiol.* 7:116. <https://doi.org/10.3389/fphys.2016.00116>
30. Huang CN, Tian XB, Jiang SM, Chang SH, Wang N, Liu MQ, Zhang QX, Li T, Zhang LJ, Yang L (2020) Comparisons between infectious and autoimmune encephalitis: clinical signs, biochemistry, blood counts, and imaging findings. *Neuropsychiatr Dis Treat* 16:2649–2660
31. Lins H, Wallesch CW, Wunderlich MT (2005) Sequential analyses of neurobiochemical markers of cerebral damage in cerebrospinal fluid and serum in CNS infections. *Acta Neurol Scand* 112:303–308
32. Martiszus BJ, Tsintsadze T, Chang W, Smith SM (2016) Enhanced excitability of cortical neurons in low-divalent solutions is primarily mediated by altered voltage-dependence of voltage-gated sodium channels. *Elife*. 2021;10. <https://doi.org/10.7554/elife.67914>.
33. Lindner JS, Rajayer SR, Martiszus BJ, Smith SM (2022) Cinacalcet inhibition of neuronal action potentials preferentially targets the fast inactivated state of voltage-gated sodium channels. *Front Physiol* 13:1066467
34. Hu W, Bean BP (2018) Differential control of axonal and somatic resting potential by voltage-dependent conductances in cortical layer 5 pyramidal neurons. *Neuron* 97:1315–1326.e1313
35. Lu B, Zhang Q, Wang H, Wang Y, Nakayama M, Ren D (2010) Extracellular calcium controls background current and neuronal excitability via an UNC79-UNC80-NALCN cation channel complex. *Neuron* 68:488–499
36. Ma Z, Siebert AP, Cheung KH, Lee RJ, Johnson B, Cohen AS, Vingtdeux V, Marambaud P, Foskett JK (2012) Calcium homeostasis modulator 1 (CALHM1) is the pore-forming subunit of an ion channel that mediates extracellular Ca²⁺ regulation of neuronal excitability. *Proc Natl Acad Sci U S A* 109:E1963–1971
37. Frankenhaeuser B, Hodgkin AL (1957) The action of calcium on the electrical properties of squid axons. *J Physiol* 137:218–244
38. Li B, Suutari BS, Sun SD, Luo Z, Wei C, Chenouard N, Mandelberg NJ, Zhang G, Wamsley B, Tian G, Sanchez S, You S, Huang L, Neubert TA, Fishell G, Tsien RW (2020) Neuronal inactivity co-opts LTP machinery to drive potassium channel splicing and homeostatic spike widening. *Cell* 181:1547–1565.e1515
39. Burgo A, Carmignoto G, Pizzo P, Pozzani T, Fasolato C (2003) Paradoxical Ca²⁺ rises induced by low external Ca²⁺ in rat hippocampal neurones. *J Physiol* 551:11
40. Sheraziya MG, von Bohlen Und Halbach O, Unsicker K, Egorov AV, (2009) Spontaneous bursting activity in the developing entorhinal cortex. *J Neurosci* 29:12131–12144
41. Beaulieu-Laroche L, Toloza EHS, van der Goes MS, Lafourcade M, Barnagian D, Williams ZM, Eskandar EN, Frosch MP, Cash SS, Harnett MT (2018) Enhanced dendritic compartmentalization in human cortical neurons. *Cell* 175:643–651.e614
42. Harnett MT, Xu NL, Magee JC, Williams SR (2013) Potassium channels control the interaction between active dendritic integration compartments in layer 5 cortical pyramidal neurons. *Neuron* 79:516–529
43. Magee JC, Grienberger C (2020) Synaptic plasticity forms and functions. *Annu Rev Neurosci* 43:95–117
44. Heir R, Stellwagen D (2020) TNF-mediated homeostatic synaptic plasticity: from *in vitro* to *in vivo* models. *Front Cell Neurosci* 14:565841
45. Mattheisen GB, Tsintsadze T, Smith SM (2018) Strong G-protein-mediated inhibition of sodium channels. *Cell Rep* 23:2770–2781
46. Steiger LJ, Tsintsadze T, Mattheisen GB, Smith SM (2023) Somatic and terminal CB1 receptors are differentially coupled to voltage-gated sodium channels in neocortical neurons. *Cell Rep* 42:112247
47. Carr DB, Day M, Cantrell AR, Held J, Scheuer T, Catterall WA, Surmeier DJ (2003) Transmitter modulation of slow, activity-dependent alterations in sodium channel availability endows neurons with a novel form of cellular plasticity. *Neuron* 39:793–806
48. Singh AK, Wadsworth PA, Tapia CM, Aceto G, Ali SR, Chen H, D'Ascanio M, Zhou J, Laezza F (2020) Mapping of the FGF14:Nav1.6 complex interface reveals FLPK as a functionally active peptide modulating excitability. *Physiol Rep* 8:e14505
49. Miyake S, Higuchi H, Honda-Wakasugi Y, Fujimoto M, Kawai H, Nagatsuka H, Maeda S, Miyawaki T (2019) Locally injected ivabradine inhibits carrageenan-induced pain and inflammatory responses via hyperpolarization-activated cyclic nucleotide-gated (HCN) channels. *PLoS ONE* 14:e0217209
50. Ma Z, Tanis JE, Taruno A, Foskett JK (2016) Calcium homeostasis modulator (CALHM) ion channels. *Pflugers Arch* 468:395–403
51. Wouk J, Rechenchoski DZ, Rodrigues BCD, Ribeiro EV, Faccin-Galhardi LC (2021) Viral infections and their relationship to neurological disorders. *Adv Virol* 166:733–753
52. Patrycy M, Chodkowski M, Krzyzowska M (2022) Role of microglia in herpesvirus-related neuroinflammation and neurodegeneration. *Pathogens*. 11:809. <https://doi.org/10.3390/pathogens11070809>
53. Karaba AH, Zhou W, Hsieh LL, Figueira A, Massaccesi G, Rothman RE, Fenstermacher KJ, Sauer L, Shaw-Saliba K, Blair PW, Robinson ML, Leung S, Wesson R, Alachkar N, El-Diwany R, Ji H, Cox AL (2022) Differential cytokine signatures of severe acute respiratory syndrome coronavirus 2 (SARS-CoV-2) and influenza infection highlight key differences in pathobiology. *Clin Infect Dis* 74:254–262
54. Galic MA, Riazi K, Pittman QJ (2012) Cytokines and brain excitability. *Front Neuroendocrinol* 33:116–125
55. Zipp F, Bittner S, Schafer DP (2023) Cytokines as emerging regulators of central nervous system synapses. *Immunity* 56:914–925
56. Köller H, Siebler M, Schmalenbach C, Müller H-W (1990) GABA and glutamate receptor development of cultured neurons from rat hippocampus, septal region, and neocortex. *Synapse* 5:59–64

Publisher's Note

Springer Nature remains neutral with regard to jurisdictional claims in published maps and institutional affiliations.

Submit your manuscript to a SpringerOpen® journal and benefit from:

- Convenient online submission
- Rigorous peer review
- Open access: articles freely available online
- High visibility within the field
- Retaining the copyright to your article

Submit your next manuscript at ► springeropen.com